



GIS-based statistical model for the prediction of flood hazard susceptibility

Sadhan Malik¹ · Subodh Chandra Pal¹  · Alireza Arabameri² · Indrajit Chowdhuri¹ · Asish Saha¹ · Rabin Chakraborty¹ · Paramita Roy¹ · Biswajit Das¹

Received: 10 December 2019 / Accepted: 25 March 2021 / Published online: 3 April 2021
© The Author(s), under exclusive licence to Springer Nature B.V. 2021

Abstract

At present, flood is the most significant environmental problem in the entire world. In this work, flood susceptibility (FS) analysis has been done in the Dwarkeswar River basin of Bengal basin, India. Fourteen flood causative factors extracted from different datasets like DEM, satellite images, geology, soil and rainfall data have been considered to predict FS. Three heuristic models and one statistical model fuzzy Logic (FL), frequency ratio (FR), multi-criteria decision analysis (MCDA) and logistic regression (LR) have been used. The validating datasets are used to validate these models. The result shows that 68.71%, 68.7%, 60.56% and 48.51% area of the basin is under the moderate to very high FS by the MCDA, FR, FL and LR, respectively. The ROC curve with AUC analysis has shown that the accuracy level of the LR model (AUC=0.916) is very much successful to predict the flood. The rest of the models like FL, MCDA and FR (AUC=0.893, 0.857 and 0.835, respectively) have lesser accuracy than the LR model. The elevation was the most dominating factor with coefficient value of 19.078 in preparation of the FS according to the LR model. The outcome of this study can be implemented by local and state authority to minimize the flood hazard.

Keywords Fuzzy logic · Logistic regression · Flood susceptibility · Frequency ratio · Multi-criteria decision analysis

1 Introduction

Flood, one of the most predominant environmental calamities, is defined as a situation, where water level rise is due to huge precipitation and in this manner overflow of the excess water over the flood plain (Malik, Chandra Pal, et al., 2020; Malik, Pal, et al., 2020). A major portion of the global populations lives in the flood plain areas, and they indirectly or directly depend on the flood plain; thereby, encroachment of human, modification of river, loss of ecosystem and climate change can cause a great threat (WMO, 2018). According

✉ Subodh Chandra Pal
geo.subodh@gmail.com

¹ Department of Geography, The University of Burdwan, Bardhaman, West Bengal 713104, India

² Department of Geomorphology, Tarbiat Modares University, 14117-13116 Tehran, Iran

to the WMO (2018), storms and floods around the world have caused millions of death from 1970 to 2012. Torrential rainfall has been considered as the prime factor behind the occurrences of a flood (Malik et al., 2020; Malik, Pal, et al., 2020; Minh et al., 2018). Sudan morphological changes generally occur because of flood (Balen et al., 2010; Tu et al., 2016).

Flood is one of the key crises all over the world, which has caused over one million of deaths for the periods of 1970 to 2012 (WMO, 2018), and 109 million people were affected during 1995 to 2015 resulting in economic loss of 75 billion US\$ in every year (Malik, Chandra Pal, et al., 2020; Malik, Pal, et al., 2020). It also affects the agriculture, natural ecosystem, cultural heritage, bridge, transporting network (Markantonis et al., 2013). Also, flood also transports the hazardous wastes in the modern days generated by several industries (Khosravi et al., 2019). Natural and anthropogenic reasons both are responsible behind the flood. But recent studies have indicated that the changes in climatic phenomenon have altered the nature and magnitude of the flood (Roy et al., 2020; Saha et al., 2021). Recent works have found that from the last few decades, human interventions to the natural system through urbanization, deforestation, riverside encroachment by human settlement result in progressively decreasing floodplain connectivity with river and increases in flood frequency with greater duration (Christensen & Christensen, 2003; Costache et al., 2021; Roy et al., 2020; Saha et al., 2021).

In case of Asia, near about 90% of damages were occurred by the flood (Smith, 2013), whereas tropical rivers of South Asia experience frequent flood event (Chowdhuri, Pal, & Chakraborty, 2020a, 2020b; Mirza, 2011). In case of India, there is no exemption to this phenomena and thereby became the most horrible flood-affected nation following Bangladesh (Brammer, 2010). Central Water Commission of India (CWC) reported that every year 32 million population has been suffering from floods due to nearly 7.21 million hectares of land inundation (Kale, 2014). Along with this, the devastating flood of Mumbai (in 2005), Jammu and Kashmir (in September 2014), Uttarakhand (in June 2013) is one of the few examples of devastating floods in India. Previous studies have concluded that flood cannot be eliminated (Bandyopadhyay et al., 2016; Huang et al., 2008). Therefore, assessment of FS and its management is very much essential to understand the flood-affected areas to reduce flood damages by considering some proper suitable measurements (Hagen & Lu, 2011).

2 Literature Reviews

Geographic information system is recognized as very significant tool for data analysis and management (Falah et al., 2019; Rahmati et al., 2016). FS mapping is an important part of predicting and managing impending floods (Falah et al., 2019; Kourgialas & Karatzas, 2011). Several approaches have been applied to predict the FS of an area (Solomatine & Ostfeld, 2008), e.g., (Al-Juaidi et al., 2018) used LR model; (Souissi et al., 2020; Swain et al., 2020) used analytical hierarchy process in GIS platform; Haghizadeh et al. (2017) used Shannon's entropy model; (Rahmati, Pourghasemi, et al., 2016; Tehrany et al., 2014) applied support vector machine and WoE; (Lee et al., 2017) used random forest and boosted regression trees; (Chowdhuri, Pal, & Chakraborty, 2020a, 2020b) used evidential belief function; (Mukerji et al., 2009) applied neuro-fuzzy, neuro-GA and ANN models; and (Najafzadeh & Zahiri, 2015) and (Zahiri & Najafzadeh, 2018) used an adaptive

learning network to estimate river discharge and floodplain modeling and many more. Apart from this, several hydrological models were also applied for flood inundation mapping (Costabile & Macchione, 2015; Malik & Pal, 2020a; Zheng et al. 2018). So, it can be said that numerous scholars have come out with their methods for FS mapping. Although lots of methods are available for FS mapping (Wheater et al., 1993), each method has its specific negative and positive aspect (Tehrany & Kumar, 2018). Thus, it became somewhat confusing to understand the top suitable and globally satisfactory methods for FS analysis (Tehrany & Kumar, 2018). Among several groups of FS mapping model, FL, MCDA, FR, decision trees (DT), LR, artificial neural network (ANN) and machine learning (ML) are the most popular models (Lee et al., 2017). The available popular methods are divided into four categories, e.g., quantitative, qualitative, hydrological and machine learning method (Arabameri, Karimi-Sangchini, et al., 2020; Arabameri, Saha, et al., 2020; Pradhan & Youssef, 2011; Rahmati, Pourghasemi, et al., 2016; Rahmati, Zeinivand, et al., 2016; Saha et al., 2021). Besides this, database requirement in hydrological model implementation, calibration and verification are not easily available in data scarcity area and for developing countries, these models are very complex in nature (Falah et al., 2019). Therefore, application of freely available datasets like digital elevation data, rainfall information and remotely sensed datasets in GIS environment has become more popular.

So, on the one hand, as we have mentioned earlier, FS mapping is very important to the government agencies, academicians, policymakers and people associated with the flood-affected areas, and on the other hand, several FS models are available to execute this. Therefore, the application of multiple FS models and their comparative assessment are very much significant to develop the FS maps. In this study, our main objective is to develop the FS maps based on MCDA, FL, FR and LR to assess the reliability of the particular models in forecasting the FS area.

3 Materials and Methods

Reliable FS map and its accuracy relied on the scale and convenience of the information as well on the models which have been applied to generate this map (Chapi et al., 2017; Mind'je, 2019a). Therefore, based on the previous studies, LULC map, soil map, geological map, rainfall and DEM have been considered (Table 1) to predict the FS. All the FS parameters have been divided following the natural breaks method offered by ArcGIS software for further analysis. Four models, such as FL, MCDA, FR and LR models, have been applied to address the FS map. Therefore, the applied models were categories into two major approaches, i.e., heuristic and statistical model. The heuristic model is the model in which rank-based weights are assigned according to its importance in that particular event, for example FL, MCDA and FR models, whereas statistical models are those, where based on the statistical analysis weights are being given as in case of LR model. Assessments of these methods and its validation have been determined through statistical measures to predict best suitable models. Detailed flowcharts are given in Fig. 1 to show the steps and procedure of this study to develop the FS maps of a study area.

3.1 Study Area

The Dwarkeswar River basin (DRB) of the West Bengal has been selected as the study area, and it is located within the Bengal basin. According to the RMSI report on India

Table 1 Detail list of data applied for the present study and its sources

Data	Type	Period / Time	Source
Flood inventory map	Maps of flooded area	2000 to 2018	Department of Irrigation and Waterways, Govt. of West Bengal (DoIW-GoWB), Dartmouth Flood Observatory (DFO) (http://floodobservatory.colorado.edu/ Version3/080E030Nv3.html)
DEM (digital elevation map)	Shuttle radar Topography mission (SRTM) Spatial resolution 30 m	2010	http://earthdata.nasa.gov/nasa-shuttle-rader-topography-mission-srtm-version-3-0-global-1-arc-second-data-released-over-asia-and-australia
Rainfall	Monthly rainfall	2000–2018	www.imd.gov.in/
Geological map	District resource map	Published in 1975–1976	Geological Survey of India
Soil map	District soil map	Published in 2015	NBSS&LUP
Land use and land cover	Land use and land cover map	Published in 2010	Geospatial Gateway from Bhuban ISRO (https://bhuvan.nrsc.gov.in/)
Drainage network	Topographical map (Scale 1:50,000)	Published from 1975 to 1984	Survey of India (SOI)
Satellite images	Landsat8 OLI/TIRS; spatial resolution 30 m	03/10/2019, spatial resolution 30 m	https://landsat.usgs.gov/

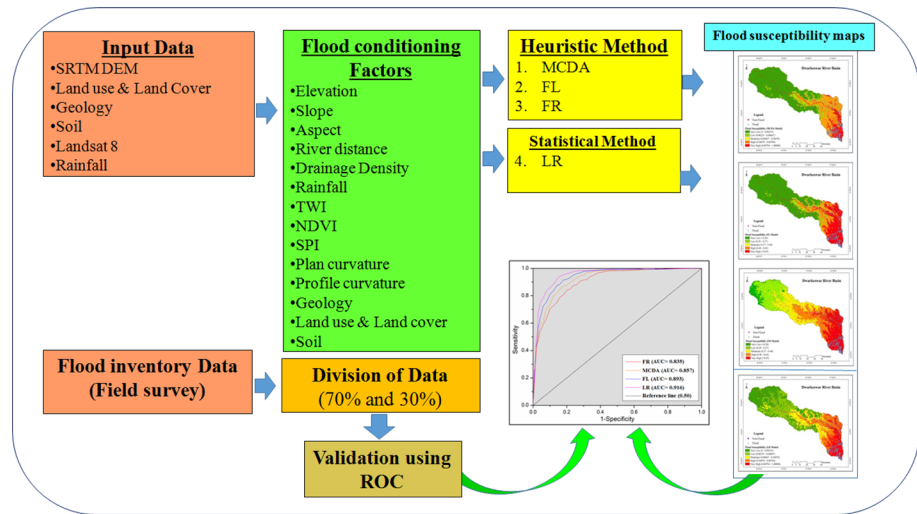


Fig. 1 Methodological framework of the study showing detailed process of flood susceptibility mapping and its validation processes

Flood Risk, Gangetic plain and West Bengal were under the extreme flood risk zone (RMSI, 2015). According to the Disaster Risk Index of States and Flood Hazard Index, in both cases, West Bengal stands second in India (Thakur and Chauhan, 2018). West Bengal is primarily an agrarian state with high population density in the low-lying alluvial region; this flood problem has become jeopardized. Irrigation and Waterways Department (IWD) of Govt. of West Bengal (Irrigation and Waterways Directorate Govt. of West Bengal, 2016) in their several reports has stated that 42 percent area of the state is prone to flood, whereas (Kale, 2003a, 2003b) argued that approximately twenty million (55.8%) of the region is susceptible to flood. (Kadam & Sen, 2012) and (Chapman & Rudra, 2007) concluded that during the September 2000 flood (Table 2), twenty million people were affected. Although several measures were taken by the Government to prevent the floods, still every year the lower part of the east-flowing rivers of the western part of the West

Table 2 Historical account of floods and its affected area of West Bengal

Flood-affected area (Sq. Km.)	Year of flood occurrence	Total number of Years
< 500	1985, 1989, 1992, 1994, 1997, 2001, 2005, 2006, 2013 and 2014	10
500–2,000	1962, 1963, 1964, 1965, 1966, 1972, 1975, 1996, 2003, 2004, 2007, 2009, 2011 and 2015	14
2,000–5,000	1960, 1961, 1967, 1969, 1970, 1974, 1976, 1980, 1981, and 1982	10
5,000–10,000	1973, 1977, 1993, 1995, 1998 and 2008	6
10,000–15,000	1968, 1979, 1983, 1990 and 1999	5
15,000–20,000	1971, 1986, 1987, 1988	4
> 20,000	1978, 1984, 1991 and 2000	4

Source: Irrigation and waterways department, Annual flood report (AFR), 2016

Bengal has been suffering from floods (Malik & Pal, 2020a). So, in this DRB enormous loss of economy, agriculture, biotic habitat and social stability has been observed by the floods and its surrounding regions historically (Table 2).

Dwarkeswar River is identified as Dhalkishore (SOI, 1978). It is one of the major rivers in the Bengal basin. The river basin is located within $87^{\circ}47'58''\text{E}$ to $86^{\circ}31'08''\text{E}$ longitude and $23^{\circ}40'25''\text{N}$ to $23^{\circ}32'00''\text{N}$ latitude (Fig. 2), covered an area of 4356.6 sq. km. It originates near Tilboni hill of Chhotonagpur Plateau in Puruliya district (O'Malley, 1995). After originating from *Panjoniya* or locally named as *Dungru*, tributaries like BekoNala, Berai, Arkasha, Dangra Nala, Kumari Nala, Shankari, Futuari Nala, Dudhbaiya Nala, etc., discharge its water in Dwarkeswar River. Near Ghatal town, Dwarkeswar River meets with Shilabati River and finally forms the Rupnarayan River (O'Malley, 1995). The elevation of the Dwarkeswar River ranges between 438 and 10 m (Fig. 2) with monotonous rolling topography and scattered residual hills of hard rock sometimes devoid of vegetation.

The lower part of the study area is sufferers from repeated flooding. I&W Dept. has stated that poor drainage condition is responsible for such frequent flood. Three river gauge stations have been found along this river, among which one gauge station is placed near Bankura Town, which is located in the upper part of the river basin. The previous records from 1978 to present have been indicated that river flow height crossed the EDL six times near the Arambag station. Apart from this, the nature of river flow is flashy.

Having a subtropical nature of climate, the study area is a dry region. The river dries up in the hot and cold periods. Geologically, the higher part of this region consists of Chhotonagpur Granite Gneiss Complex which belongs to the Proterozoic age. The central part of this river basin is associated with the Cainozoic Laterite. Holocene Sediment is found in the lower part of the river basin (GSI 1999). The spatial pattern of this river

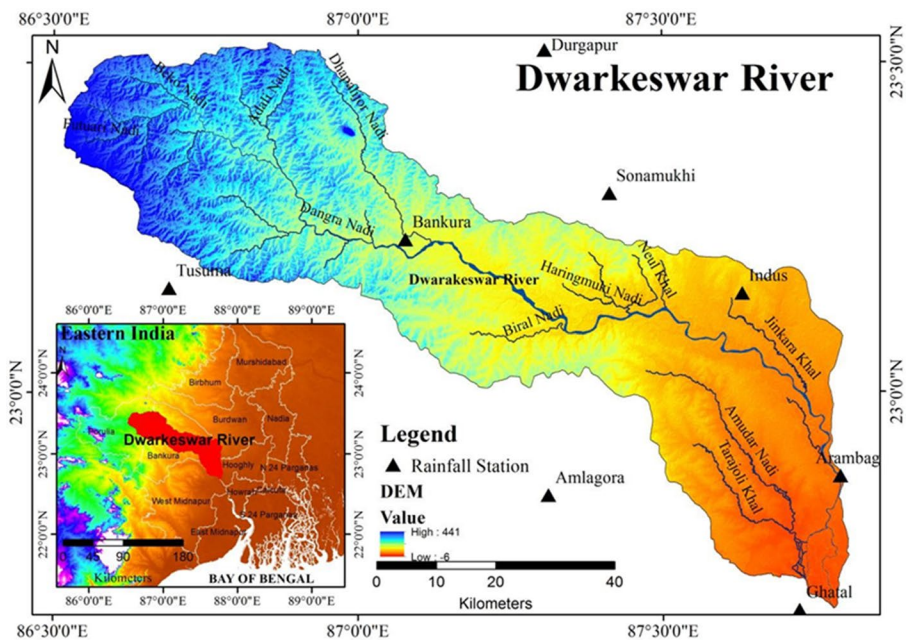


Fig. 2 Location map of the study area showing administrative location, drainage network and distribution of elevation

basin is elongated in nature (Fig. 2). Maximum length and width of the drainage basin are 159.84 km and 40.80 km, respectively. The total extent of the main trunk stream is 228.65 km. Bifurcation ratio of the river basin always exceeds 3 (Table 3); thereby, it is very much prone to flood (Strahler, 1957).

3.2 Flood inventory mapping

Historical documentation of flood-prone areas is known as flood inventory (FI) data, which is generally prepared based on previous records (Pourghasemi & Beheshtirad, 2015). FI map is very much useful to predict the future flood (Rahmati, Pourghasemi, et al., 2016; Rahmati, Zeinivand, et al., 2016). However, its reliability markedly relies on the spatial and temporal extent of flood record. In this study, FI map has been prepared applying 1400 (700 each for non-flood and flood) points from the study area extracted from Dartmouth Flood Observatory (DFO) and IWD, Govt. of West Bengal for the period of 2000–2018. Flood points have been validated through field survey. Entire dataset was divided into 70/30 ratio, in which 70% of the dataset has been selected randomly to run the model and remaining part has been used in validation (Fig. 1).

3.3 Flood susceptibility factors

Here, 14 flood causative factors have been incorporated on the basis of earlier works (Table 4 and Fig. 3) incorporating TWI, NDVI, elevation, aspect, slope, PIC, DD, PrC, distance from river, rainfall, LULC, SPI, geology and soil. Selected factors are very significant for assessing and delineating of FS regions of any area.

3.3.1 Elevation

Elevation has been considered as an important aspect in FS assessment. Also, lower altitude is generally associated with flood-prone areas (Roy et al. 2020). The relationship between FS and elevation is inversely related to the elevation (Malik, Chandra Pal, et al., 2020; Malik, Pal, et al., 2020), thereby indicating that areas associated with very low altitude may experience a severer flood. So, it is the most important variable to estimate FS. Here, the elevation map was created from SRTM data with 30 m spatial resolution (Fig. 3a).

Table 3 Drainage basin and network properties of the Dwarkeswar River

Stream order	No. of stream	Basin area (Km ²)	Length of the stream (km.)	Bifurcation ratio
1	1073	4.35	1.11	
2	280	9.43	2.19	3.83
3	62	34.65	6.36	4.52
4	17	116.17	14.3	3.65
5	3	694.28	31.07	5.67
6	1	4356.72	152.19	3.00

Source: Topographical maps (Published by Survey of India)

Table 4 Multi-collinearity test of flood conditioning factors

Flood conditioning factors	Multi-collinearity statistics	
	Tolerance	VIF
Aspect	0.967	1.034
River distance	0.504	1.983
Drainage density	0.46	2.174
NDVI	0.825	1.212
SPI	0.524	1.908
Elevation	0.236	4.239
Rainfall	0.772	1.296
Wetness index	0.466	2.148
Plan curvature	0.631	1.586
Profile curvature	0.702	1.425
Slope	0.475	2.103
Land use and Land cover	0.932	1.073
Geology	0.28	3.577
Soil	0.537	1.864

3.3.2 Aspect

Aspect is an major attribute to predict the FS (Mind'je et al., 2019; Tang et al., 2020; Tehrany et al., 2015). It is the maximum slope direction (Choubin et al., 2019). The aspect map of the study area was generated from the DEM in Arc GIS software (Fig. 3b).

3.3.3 Distance from the river

It is a vital parameter to determine the FS (Choubin et al., 2019). Due to excessive and storm rainfall in a drainage basin, channel flow increases and when it crosses the limits of the channel capacity, it turns into flood. Therefore, nearer to the river, FS is more and away from the river, FS decreases. It has been estimated in the ArcGIS software from the extracted drainage network of DEM and topographical maps (Fig. 3c).

3.3.4 Drainage density

It is defined as the length of drainage per unit area (Horton, 1932). In a drainage basin, concentrated flow occurred after rainfall and subsequently, when the channel flow crosses the limits of channel capacity, its excess water overflows in the adjacent area and creates a flood. Therefore, it is one of the key aspects in the assessment of the FS of any area (Arabameri, Karimi-Sangchini, et al., 2020; Arabameri, Saha, et al., 2020). Topographical maps from the Survey of India in association with DEM (Fig. 3d) were used to demark stream network. After that, DD has been computed by the line density tool available in the ArcGIS.

3.3.5 Estimation of Normalized Difference Vegetation Index (NDVI)

NDVI is an index of vegetation status, which indicates the phenomenological nature of the vegetation. This index can help to identify the FS area (Kumar & Acharya, 2016; Paul et al., 2019). NDVI was calculated from the Landsat8 OLI/TIRS Eq. (1) (Fig. 3e).

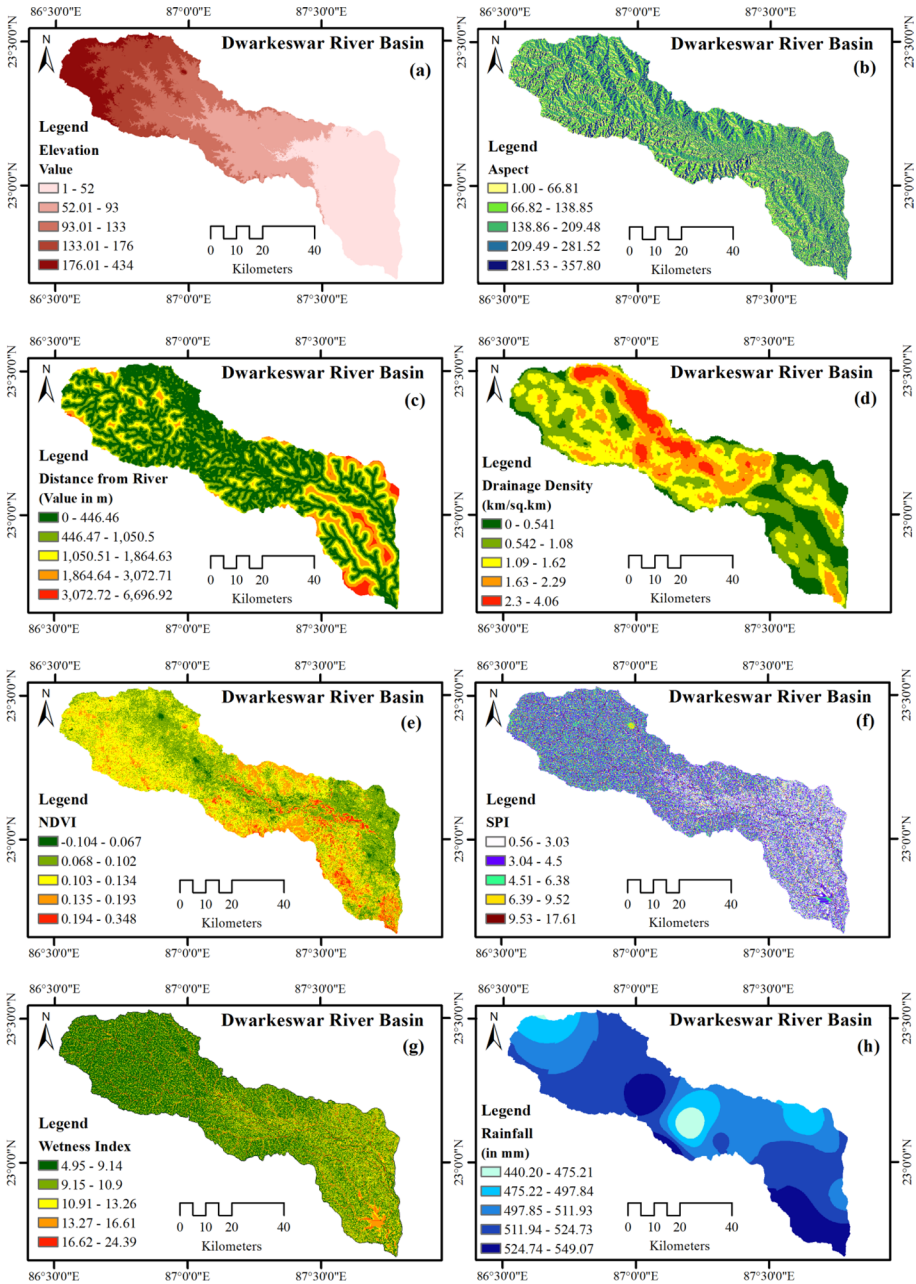


Fig. 3 Flood susceptibility factors and its spatial variation in the study area such as **a** elevation, **b** aspect, **c** distance from river, **d** drainage density, **e** NDVI, **f** stream power index, **g** wetness index, **h** rainfall, **i** plan curvature, **j** profile curvature, **k** slope, **l** geology, **m** soil and **n** land use and land cover

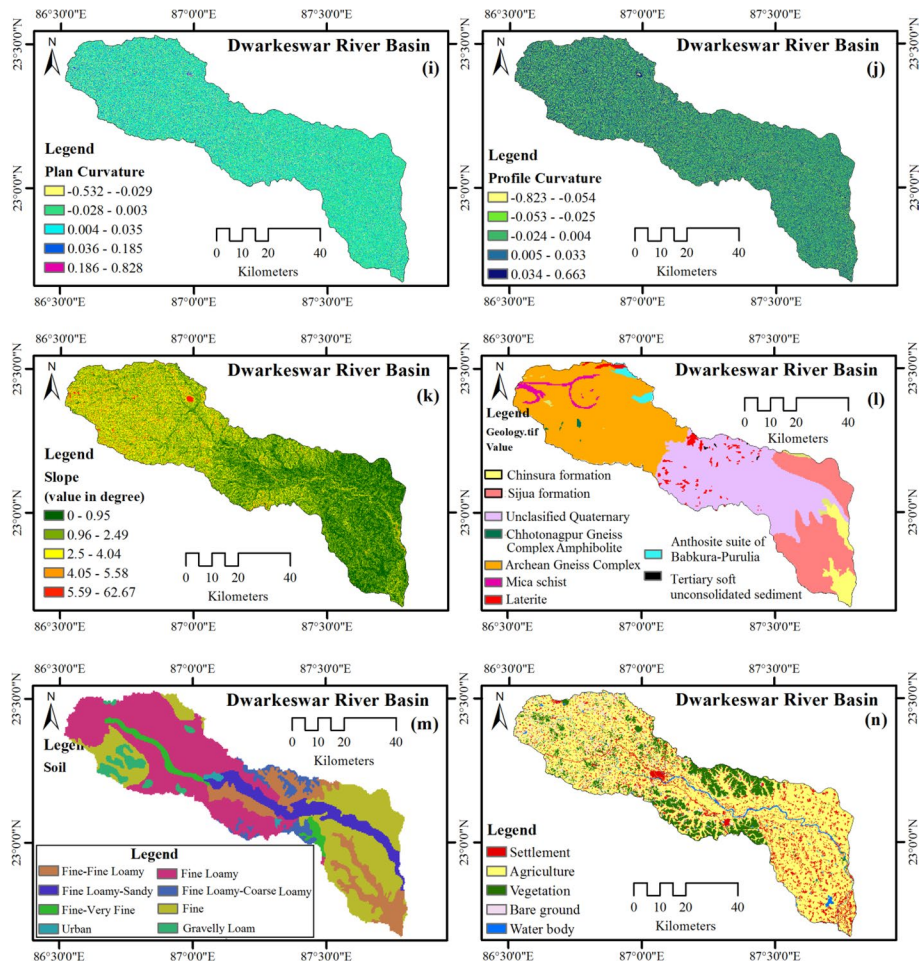


Fig. 3 (continued)

$$NDVI = \frac{(NIR - RED)}{(NIR + RED)} \tag{1}$$

where NIR represents near infrared band (Band no 5 for Landsat8 OLI/TIRS) and RED indicates band no 4 for Landsat8.

Nature of vegetation changes in response to variations in geomorphology, and thereby, the flood plain vegetation is different from other kinds of vegetation. In this way, it is very much helpful to predict the FS area.

3.3.6 Stream Power Index

Stream power index or SPI represents the intensity of the surface runoff and potentiality of erosion (Termeh et al. 2018). High amount of SPI indicates the greater ability of surface runoff, and low amount of SPI denotes the poorer surface runoff. Thus, substantial rainfall

may lead to the flood in the low SPI area. In this study, it was calculated in the ArcGIS platform applying SRTM DEM using Eq. (2) (Fig. 3f).

$$\text{SPI} = A_s \times \tan \beta \quad (2)$$

where SPI represents stream power index; specific basin area (in m^2) represented by A_s and β represents the slope (in degree). It was applied by several researchers to estimate the FS (Saha et al., 2021).

3.3.7 Topographic Wetness Index

Topographic wetness index or TWI is an important factor which was previously applied by several scholars to predict the FS of an area (Costache et al., 2021; Saha et al., 2021). Areal dispersal and saturation of surface runoff are strongly controlled by this TWI. In this research work, the TWI was computed in the GIS platform from the DEM following the given Eq. (3) (Fig. 3g).

$$\text{TWI} = \ln \left(\frac{A_s}{\tan(\text{slope})} \right) \quad (3)$$

where A_s represents the specific catchment area (m^2m^{-1}) and the slope has been measured in degree. Preceding research works display that FS and TWI are related positively to each other (Saha et al., 2021). Thus, this indicator is very good to determine the proneness of the flood.

3.3.8 Rainfall (mm)

Rainfall is the greatest significant parameter for FS mapping (Costache et al., 2021; P. Roy et al., 2020; Saha et al., 2021). The upper part of the study area is characterized by semiarid climate and very small rainfall, while the lower and middle part is associated with a monsoon climate. Monthly rainfall data for all the selected stations from IMD were collected for the period of 2000–2018 and interpolated in the ArcGIS environment to extract the basin rainfall (Fig. 3h). Several previous studies strongly argued that positive relationships exist between rainfall and flood (Bandyopadhyay et al., 2016; Chowdhuri & Chakraborty, 2020a, 2020b; Das et al., 2018). So huge rainfall is strongly associated with a greater probability of flood occurrence, and in opposite situation, it is devoid of flood occurrence.

3.3.9 Plan Curvature

It is important factor in detecting the FS (Lee et al., 2012; Paul et al., 2019), and it represents vertical to the slope bearing. A negative value indicates the concave profile, whereas zero denotes the flats surface and positive value represents the convex profile. It influences the runoff, and thereby, it will provide fruitful insight into the FS prediction. It has been generated from DEM using ArcGIS platform (Fig. 3i).

3.3.10 Profile Curvature

The curvature of terrain in the slope direction is called profile curvature. This can determine significant control over the surface runoff. In this way, it will provide a significant

indication of FS assessment (Arabameri et al. 2019). Profile curvature has been computed in the ArcGIS environment using Arc tool from the DEM (Fig. 3j). Profile curvature is also similar to the plan curvature in terms of nature of profile and its representing value (Fig. 3j).

3.3.11 Slope

Slope determines the nature and strength of water stagnation and water percolation (Rahmati, Pourghasemi, et al., 2016; Rahmati, Zeinivand, et al., 2016). It is also negatively related to the flood. Heavy rainfall on the surface with extremely low slope is accompanied with very low surface runoff velocity, water inundation and thereby floods (Rahmati, Pourghasemi, et al., 2016). Besides the same situation with moderate-to-high slopes subjected to a higher rate of runoff and thereby less vulnerable to flood, slope map was prepared from the 30 m SRTM DEM data in the ArcGIS software (Fig. 3k).

3.3.12 Geology

A varying geological character of a river and its basin can determine the nature of infiltration, channel properties and runoff generation (Miller et al., 1990) and thereby can indicate the FS of a river basin (Sahana & Patel, 2019). Earlier research works have also discussed the significance of the geological factor in the assessment of FS of an area (Table 4) (Khosravi et al., 2019; Lee et al., 2017; Malik & Pal, 2021). Consequently, the geological aspect was incorporated to formulate the FS map of the DRB. This datum from GSI was collected, and nine geological components were identified (Fig. 3l).

3.3.13 Soil

It is another flood contributing factor. Surface runoff properties and thereby flood peak are determined by infiltration rate of soil (Chen et al. 2020). Apart from this, types of soil are also influenced by the floods and its deposits. So, soil type carries a significant indication for FS. Past literature also indicates that soil is an important aspect in the FS mapping (Ganguly et al., 2008; P. Roy et al., 2020; Saha et al., 2021) (Table 4). Soil maps of all corresponding districts were collected from NBSS&LUP. Eight types of soil are observed in the Dwarkeswar River (Fig. 3m).

3.3.14 Land Use and Land Cover (LULC)

Evapotranspiration, infiltration and runoff are generally influenced by the LULC of an area (Kadam & Sen, 2012; Kumar & Acharya, 2016; Rahmati, Pourghasemi, et al., 2016; Rahmati, Zeinivand, et al., 2016). So, it directly or indirectly influences the FS of an area. Literature review on FS parameters (Table 4) indicates that most of the scholars have incorporated LULC to predict FS in their studies. In this study, LULC map was collected using Bhuvan's Geospatial Gateway from Indian Space and Research Organization (ISRO) (Table 1). Five categories of LULC were considered, such as agriculture, bare ground, settlement, water body and vegetation (Fig. 3n).

3.4 Multi-collinearity Test

Multi-collinearity test has been used in this study to eliminate the related factors from the model to reduce the possible chance of error, where the tolerance and variance inflation factor (VIF) act as an important part to identify the inaccuracy. The tolerance and VIF have been calculated in the following given formulas 4 and 5.

$$\text{Tolerance} = 1 - r^2 \quad (4)$$

$$\text{VIF} = 1/\text{Tolerance} \quad (5)$$

where tolerance level < 0.1 and VIF results > 10 represent multi-collinearity issue (Khosravi et al., 2019). In this study, less than 5 VIF value has been considered to judge the parameters for FS modeling.

3.5 Flood susceptibility mapping

Several popular FS models exist (Dottori et al., 2018). But considering data availability and suitable of approaches, four popular models such as FZ, MCDA, LR and FR have been used for FS analysis. A detailed description of these models has been described below.

3.5.1 Multi-criteria Decision Analysis (MCDA)

It was prepared by Saaty in 1977. MCDA is one of the most popular methods of heuristic analysis (Malik et al., 2019). Pairwise comparisons were done to reach some logical conclusion (Fernández & Lutz, 2010). Pairwise disintegration, amalgamation and comparison of priorities are the basic principle behind this model (Malik et al., 2019). Several research works following this model have been done to estimate FS (Rahmati, Pourghasemi, et al., 2016; Rahmati, Zeinivand, et al., 2016). It was used in a numerous perspectives to achieve the required goal, for example, gully erosion vulnerability, groundwater valuation (Chakraborty et al., 2018), gold assessment (Madani, 2011), landslide susceptibility (Ma et al., 2019; Yilmaz, 2010), flood vulnerability (Dano et al., 2019; Nachappa et al., 2020) and so on. In the case of developing nations and the area which is lacking of adequate information, this model is very much helpful. Consistency ratio (CR) is very important to evaluate the factors (Ergu et al., 2011), which provide the decision to be accepted only if the $\text{CR} = > 0.10$. It was computed using the given Eq. (6):

$$\text{CR} = \text{CI}/\text{RI} \quad (6)$$

Here, RI is the random index and CI denotes consistency index which were derived from the number of parameters (n). CI is calculated using Eq. (7).

$$\text{CI} = (\lambda \max - n)/(n - 1) \quad (7)$$

Here, $\lambda \max$ represents the highest eigenvalue in the data matrix. Therefore, successful application of the MCDA model in association with GIS has been used to assess the FS of the study area. In a systematic manner, a priority matrix was prepared on the basis

of pairwise comparison of the selected parameters and their subtheme keeping CR value to 0.045. After that, all the parameters had been incorporated in the weighted overlay tool in ArcGIS to assess the FS of the study area using the given formula 8.

$$\begin{aligned} \text{FSusingMCDA} = & \{ (E_w \times E_{wi}) + (DI_w \times DI_{wi}) + (DR_w \times DR_{wi}) + (DD_w \times DD_{wi}) \\ & + (NDVI \times NDVI_{wi}) + (SPI \times SPI_{wi}) + (A_w \times A_{wi}) + (R_w \times R_{wi}) \\ & + (TWI_w \times TWI_{wi}) + (RR_w \times RR_{wi}) + (PIC_w \times PIC_{wi}) \\ & + (PrC_w \times PrC_{wi}) + (Sl_w \times Sl_{wi}) + (G_w \times G_{wi}) + (So_w \times So_{wi}) \\ & + (L_w \times L_{wi}) \end{aligned} \quad (8)$$

where FS—flood susceptibility, MCDA—multi-criteria decision analysis, DR—distance from the river—elevation, DI—dissection index, E —elevation, DD—drainage density, SPI—stream power index, NDVI—normalized differential vegetation index, R —rainfall, A —aspect, RR—relative relief, TWI—topographic wetness index, PrC—profile curvature, PIC—plan curvature, So—soil, Sl—slope, L—LULC, w —weight of the theme and w_i —weight of the individual classes.

3.5.2 Fuzzy Logic

Fuzzy logic or FL is an additional popular model to determine the FS of any region (Pulvirenti et al., 2011). It was presented by (Zadeh, 1965) to processes difficult problems (Zimmermann, 1996) in a simple manner. It comprises of three main portions, for example, fuzzification, defuzzification and fuzzy inference (Nandalal & Ratnayake, 2011). Membership value of this model ranges from 0 to 1. If the set of the situation is affirmative, then the value will be 1; on the other hand, it is 0 for non-members. So, it is a quantitative form of belief for a particular variable. Determination of fuzzy membership is not bound by strict laws (Ray et al., 2007). In this study, normalized value for fuzzy membership has been obtained from analytical hierarchy processes following (Saaty, 1977) and it has been applied for fuzzy membership function to reduce the biases in the model and result. Fuzzy index map was generated applying 14 selected factors. Fuzzified index maps were generated applying if-then policy in the GIS environment. After that, computed fuzzy index maps were incorporated through given Eq. (9).

$$\mu_{\text{combination}} = \text{MAX}(\mu_A, \mu_B, \mu_C, \mu_A \dots) \quad (9)$$

where A, B, C represent selected theme.

3.5.3 Frequency Ratio (FR)

The FR is a popular probability method usually used for prediction performance analysis (Saro Lee & Sambath, 2006). In a wider sense, the probability of an event to the probability of non-event phenomenon for selected variables has been estimated through FR method (Bonham-Carter, 1994). This approach is based on the experimental relationship among the occurrence of floods and flood-related several conditioning factors. This is because of revealing the inter-relationship between the flood points and various conditioning factors for a particular area. FR model has been used in various fields for a long time with optimal

precision result such as in landslide (S. Pal & Chowdhuri, 2019), gully (Arabameri, Pradhan, & Lombardo, 2019a, 2019b), flood (Samanta et al., 2018), susceptibility analysis and more. The value of FR has been calculated based on the ratio between percentage of flood pixel and percentage of total area pixel of respective factor's classes. If the value of FR is > 1 and < 1 , then it means higher and lower correlation among the flood occurrences and factors classes, respectively (Mandal et al., 2018). Equation (10) was used to calculate FR.

$$FR = \frac{(NF_{pix} / \sum_{i=1}^n NF_{pix}) \times 100}{(NC_{pix} / \sum_{i=1}^n NC_{pix}) \times 100} \quad (10)$$

where FR represents frequency ratio value, NF_{pix} indicates number of flood pixel in a respective factor's class, $\sum_{i=1}^n NF_{pix}$ indicates summation of all flood pixels in the total area, NC_{pix} indicates number of pixel of respective factor's class, and $\sum_{i=1}^n NC_{pix}$ indicates summation of all pixel class in the total area.

3.5.4 Logistic Regression

Logistic regression (LR) is universally accepted widespread numerical method to estimate the FS (Mind'je et al., 2019a; Shafapour Tehrany et al., 2019). LR method is very much useful for the analysis of multiple independent factors of an event (Chowdhuri, Pal, & Chakraborty, 2020a, 2020b). Therefore, the LR method has been applied to assess the FS from the following given Eq. (11).

$$\begin{aligned} FS = & V_0 + \text{Elevation} \times W_1 + \text{Slope} \times W_2 + \text{Drainage density} \times W_3 \\ & + \text{Aspect} \times W_4 + \text{Plan curvature} \times W_5 + \text{Profilecurvature} \times W_6 \\ & + \text{Distancefromriver} \times W_7 + \text{NDVI} \times W_8 + \text{SPI} \times W_9 + \text{Rainfall} \\ & \times W_{10} + \text{TWI} \times W_{11} + \text{LULC} + \text{Soil} + \text{Geology} \end{aligned} \quad (11)$$

where y —dependent variables or FS; V_0 —the intercept of the model; and $W_1 \dots W_n$ —partial regression coefficients. In this study, 70% data were selected randomly to execute the model. In this, LR has been analyzed in the SPSS software and coefficients for individual themes of the LR have been derived and the possibility of incidence was calculated by the given calculation number 12 and concluding vulnerability for flood map has been obtained.

$$P = 1/(1 + e^{-y}) \quad (12)$$

where e —linear amalgamation of reliant parameters; P —is the probability of occurrence.

3.5.5 Model validation

The model validation of models and maps is an important aspect to test the reliability of a model or models. In this regard, AUC and ROC are considered as one of the best indicators to assess the models (Band et al., 2020; Pal et al., 2020). Besides, it was widely used in Earth Science and geo-spatial modeling (Arabameri et al., 2020; Arabameri, Saha, et al., 2020; Chowdhuri et al. 2020a, 2020b). The quantification of successful events and non-successful event and plotting of sensitivity and 1-specificity on the abscissa and ordinates, respectively, are the key aspect of it (Pourghasemi & Rahmati, 2018). Here, four models

have been selected to estimate the FS and thereby comparative analysis of the applied models applying the given formula 13

$$\text{AUC} = \frac{\sum \text{TP} + \sum \text{TN}}{P + N} \quad (13)$$

where TN or true negative is the classified non-flood pixel; TP or true positive is the categorized flood pixel; P is the sum of flood points; and N is the sum of non-flood points.

The value of AUC between 0.5 and 1.0 is considered as the best-fitted model (Yesilnacar & Topal, 2005; Yilmaz, 2010). In this study, 30% data were not incorporated to run the model and were considered as points for validation.

4 Result and analysis

Flood susceptibility map using AHP, FL, KD and LR was computed individually, and the result is given below.

4.1 Multi-collinearity test

Here, after literature review, several flood causative factors have been selected and the numbers of factors have been decreased to fourteen once successful multi-collinearity tests with less than 5 VIF value (Table 4).

4.2 Analysis of flood susceptibility

FS applying MCDA, LR, FR and FL was computed individually, and the result is as follows.

4.2.1 FS using MCDA

MCDA has been applied in FS modeling for the study area. It was observed that the lower section of this river basin is extremely susceptible to flood, whereas the higher part of the basin shows extremely little to moderate FS. The FS map was classified into 5 categories, e.g., very high (>0.32), high (0.27–0.32), medium (0.20–0.27), low (0.15–0.20), and very low (<0.15) FS zone in a GIS platform. Regional exposure of the FS area and its percentage is given in Table 6. Table 6 and Fig. 4c indicate that a greater part of the basin area is associated with very high FS area (23.44%), whereas very low, low, moderate and high FS zone covers 12.37%, 18.92%, 22.99% and 22.28% area of the basin, respectively. The areas of outer margin of dissected plateau fringe area to flat alluvial plain with an elevation range from 42 to 7m are prone to high and very high FS.

4.2.2 FS using FL

FS map applying FL was computed to understand the FS mapping of the study area (Fig. 4a). Downstream section of the DRB is related to the very high (>0.32) FS area

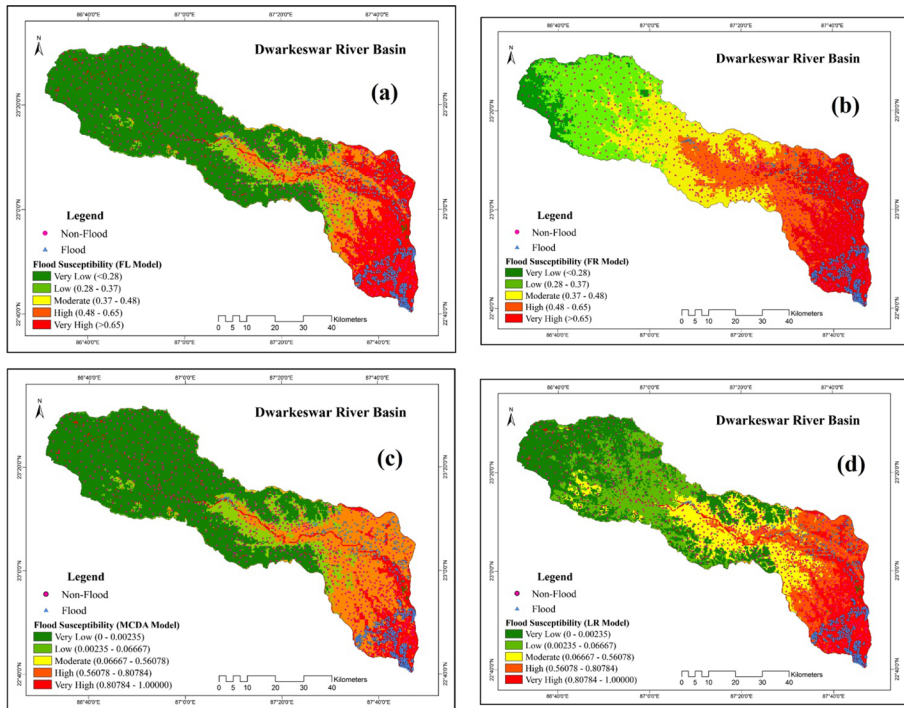


Fig. 4 Spatial variation of flood susceptibility mapping using FL (a), FR (b), MCDA (c) and LR (d)

covering 17.29% of the basin (Table 6). This area is characterized by very gentle slope and low elevation (below 36 m.). Paddy cultivation is the major economic activity of this area. The value of high FS index of this model ranges from 0.27 to 0.32 covering 23.02% area of the basin area. Moderate FS index of this model for the Dwarkeswar River varies from 0.20 to 0.27 and covers 20.25% area of the study area (Table 6). Low FS class ranges from 0.14 to 0.20 covering 19.90% area of the study area, which mainly belongs to the plateau fringe area of the basin, and its elevation varies from 80 to 434 m. Besides, below 0.14 represents very low FS index and its spatial coverage is 19.54% of the basin area (Table 6).

4.2.3 FS using FR

FR is another significant model to predict the FS of an area. In this study, another FR model was used for FS of this basin (Fig. 4b). Spatial distribution of FS index was classified into 5 parts following natural break method, such as low (<0.28), low ($0.28-0.37$), moderate ($0.37-0.48$), high ($0.48-0.65$) and very high (>0.65) (Fig. 4b). It was observed that the maximum part of the basin area is falling in the low FS category which represents 24.27% area of the study area (Fig. 4b and Table 5 and 6). The downstream section of the DRB belongs to the very high FS area and shows 24.16% of the drainage area (Fig. 4b and Table 6). It is characterized by plain alluvial land, low elevation not more than 42m and intensive agriculture, whereas very low, moderate and high FS zone covers 7.02%, 22.99% and 21.55% area of the basin area, respectively (Table 6). This result indicates that

Table 5 Flood conditioning layers, their classes and respective logistic regression coefficients

Factors	Class range	Number of pixels in domain	Pixels percentage (%)	Number of floods occurrences point	Non-floods occurrences point	Coefficients
Aspect	1.000–66.805	238,945	4.94	48	35	
	66.805–138.848	1,521,636	31.44	192	194	
	138.848–209.479	1,440,092	29.75	193	237	-0.001
	209.479–281.522	1,238,738	25.59	218	173	
	281.522–357.803	400,589	8.28	52	62	
	0.000–446.462	2,215,141	45.77	285	306	
	446.462–1050.498	1,449,026	29.94	164	200	
	1050.498–1864.634	743,062	15.35	124	125	0.271
	1864.634–3072.707	344,729	7.12	103	54	
	3072.707–6696.925	88,042	1.82	27	16	
Drainage density (km/sq.km)	0.000–0.541	801,717	16.56	211	136	
	0.541–1.083	1,430,827	29.56	162	215	
	1.083–1.624	1,463,241	30.23	157	186	0.537
	1.624–2.293	830,139	17.15	161	121	
	2.293–4.060	314,076	6.49	12	43	
	-0.171	230,322	4.76	52	30	
	0.067–0.102	1,688,471	34.89	286	234	
	0.102–0.134	2,000,309	41.33	150	314	1.167
	0.134–0.193	768,374	15.88	141	105	
	0.193–0.348	152,524	3.15	74	18	
SPI	0.560–3.034	560,584	11.58	166	76	
	3.034–4.504	2,468,240	51.00	355	360	
	4.504–6.376	1,306,926	27.00	118	187	-0.443
	6.376–9.518	408,748	8.45	50	60	
	9.518–17.607	95,502	1.97	13	18	

Table 5 (continued)

Factors	Class range	Number of pixels in domain	Pixels percentage (%)	Number of floods occurrences point	Non-floods occurrences point	Coefficients
Elevation (m)	1.000–52.000	1,688,660	34.89	640	271	
	52.000–93.000	1,020,194	21.08	23	186	
	93.000–133.000	863,493	17.84	16	112	19.078
	133.000–176.000	849,056	17.54	20	90	
Rainfall (mm)	176.000–434.000	418,597	8.65	4	42	
	440.200–475.209	118,721	2.45	2	23	
	475.209–497.837	599,537	12.39	28	93	
	497.837–511.926	1,436,697	29.68	190	194	
	511.926–524.735	2,024,261	41.82	110	303	
	524.735–549.070	660,784	13.65	373	88	
Wetness index	4.951–9.144	2,040,474	42.16	117	272	
	9.144–10.897	1,610,167	33.27	243	249	
	10.897–13.260	729,976	15.08	180	96	
	13.260–16.614	358,731	7.41	138	63	15.394
Plan curvature	16.614–24.389	100,652	2.08	24	21	
	–0.503	655,914	13.55	65	86	
	–0.032	2,207,947	45.62	359	346	
	0.003–0.035	1,409,338	29.12	205	205	18.547
	0.035–0.185	565,458	11.68	68	54	
	0.185–0.828	1343	0.03	6	10	

Table 5 (continued)

Factors	Class range	Number of pixels in domain	Pixels percentage (%)	Number of floods occurrences point	Non-floods occurrences point	Coefficients
Profile curvature	-0.769	191,580	3.96	27	29	
	-0.029	772,632	15.96	103	90	
	-0.029	1,737,951	35.91	295	269	1.643
Slope (degree)	0.004-0.033	1,458,550	30.14	198	222	
	0.033-0.663	679,287	14.03	80	91	
	0.000-0.951	1,331,095	27.50	397	212	
	0.951-2.493	2,272,980	46.96	272	359	
	2.493-4.036	970,894	20.06	22	115	0.495
	4.036-5.578	231,706	4.79	4	12	
	5.578-62.672	33,325	0.69	6	3	
	Buildup area	580,586	12.00	153	313	1.307
	Agriculture	3,312,719	68.44	184	312	7.184
	Vegetation	621,724	12.85	203	61	5.625
Soil	Barren land	212,323	4.39	115	11	0.023
	Water body	112,648	2.33	46	4	15.463
	Fine-fine loamy	660,565	13.65	124	42	9.976
	Fine loamy-sandy	422,239	8.72	38	28	7.298
	Fine loamy-coarse loamy	169,218	3.50	33	53	6.079
	Urban	26,642	0.55	134	159	5.798
	Fine loamy	1,796,492	37.12	131	144	5.493
	Fine loamy-coarse loamy	193,439	4.00	135	121	2.514
	Fine	1,415,266	29.24	105	112	3.115
	Gravelly loam	156,139	3.23	11	32	1.342

Table 5 (continued)

Factors	Class range	Number of pixels in domain	Pixels percentage (%)	Number of floods occurrences point	Non-floods occurrences point	Coefficients
Geology						
	1. Chinsura formation	188,103	3.89	89	47	16.174
	2. Sijua formation	904,433	18.69	211	51	15.952
	3. Unclassified quaternary	1,600,718	33.07	151	241	4.911
	4. Chhotonagpur gneiss complex amphibolite	7697	0.16	121	168	-1.152
	5. Archean gneiss complex	1,893,376	39.12	104	124	1.419
	6. Mica schist	37,043	0.77	5	5	-1.481
	7. Laterite	82,425	1.70	12	24	0.992
	8. Anorthosite suite of Bankura-Purulia	77,133	1.59	6	16	0.662
	9. Tertiary soft unconsolidated sediment	49,072	1.01	2	25	-0.670
						Intercept=0.314

Table 6 Results of MCDA, FR, FL and LR in the case of each factor

Class	MCDA (Sq. Km.)	MCDA (%)	FR (Sq. Km.)	FR (%)	FL (Sq. Km.)	FL (%)	LR (Sq. Km.)	LR (%)
Very low	538.99	12.37	306.01	07.02	851.31	19.54	1345.79	30.89
Low	824.39	18.92	1057.37	24.27	866.81	19.90	897.19	20.59
Medium	1001.55	22.99	1001.56	22.99	882.10	20.25	732.05	16.80
High	970.54	22.28	939.05	21.55	1003.05	23.02	727.17	16.69
Very high	1021.13	23.44	1052.61	24.16	753.33	17.29	654.41	15.02

elevation and its related aspects are the major factors behind the susceptibility of flood in this river basin.

4.2.4 FS using LR

The FS map also shows similar kinds of result compared to the earlier models. Negative weights of the different factors of the LR indicate negative relation with the occurrences of the flood, whereas positive coefficient plays a positive role in FS. It was observed that coefficients of variation of different floods inducing variables are different (Table 6). Principal coefficient values of flood inducing factors are plan curvature (18.547), elevation (19.078), TWI (15.394), water body (15.463), Sijua formation (15.952) and Chinsura formation (16.174), while modest flood-inducing variables are agriculture (7.184), fine–fine loamy soil (9.976), urban area (5.798), vegetation (5.625), fine loamy–coarse loamy (6.079), fine loamy–sandy (7.298) and fine loamy (5.493). Besides this, according to LR model, fine soil (3.115), fine loamy–coarse loamy (2.514), gravelly loam (1.342) built-up area (1.307), NDVI (1.167), profile curvature (1.643), drainage density (0.537), slope (0.495), distance from the river (0.271), barren land (0.023), aspect (−0.001), rainfall (−0.01), SPI (−0.443) and entire geological factors excluding Sijua and Chinsura formations display negative to an insignificant character in the determination of FS. Here, very high FS category is associated with extremely low spatial coverage of the basin area (15.02%) and its FS index level is above 0.808 (Fig. 4d). Similar to the preceding result, this zone of very high FS zone is characterized by extremely low altitude and its associated factors such as SI, RR and DI. The index value of high FS area ranges from 0.808 to 0.56, and it has occupied 16.69% area of the basin. Moderate FS zone covers 16.80% area of the basin, and the FS index varies from 0.067 to 0.56. Very low and low FS index varies from <0.002 and 0.002 to 0.067 and covers 30.89% and 20.59% of the DRB correspondingly.

4.3 Accuracy assessment

Here, selected models were applied to understand the FS of this area. Therefore, evaluations of these models have been done to judge the suitable models for the FS. Accuracy assessment shows that the AUC value of LR, FL, MCDA and FR was 0.916, 0.893, 0.857 and 0.835, respectively. So, it is clear that LR regression has become the best suitable method for the FS analysis of the Dwarakeswar River (Fig. 5). Figure 6 shows some snaps of flood situation.

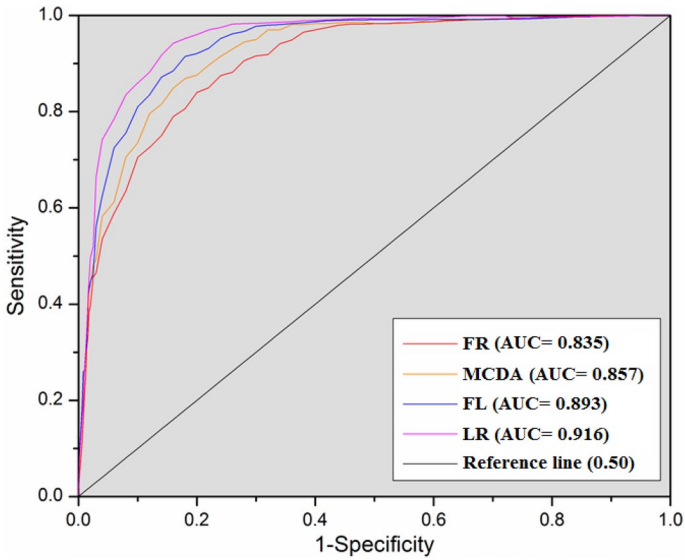


Fig. 5 Model evaluation of MCDA, FR, FL and LR using sensitivity and specificity by AUC analysis indicating higher accuracy of LR



Fig. 6 Flood-affected area **a** near Girijatala, Hooghly; **b** near Mansukha, vast agricultural field submerged under flood August 2016; **c** near Arambag, a school was affected by flood water from Dwarkeswar River during the same time and **d** near Thakurani Chak, Hooghly, where road and surrounding areas submerged under flood water

5 Discussion

Flood is a major environmental hazards, and it cannot be fully prohibited. It became more frequent with greater intensity with the growing population, human invasion and climate change. Therefore, it is very much important to understand and prepare FS map through which with a scientific assessment with proper precautions and required management policy can be formed for the respective area. In this study, FL, MCDA, LR and FR models were applied for the preparation of FS mapping of the Dwarkeswar River.

FS mapping can be defined as the area susceptible to flooding on the basis of selected responsible factors (Lin et al., 2019). However, numerous factors are accountable for the flood like relief, aspect, rainfall, drainage condition, geology, geomorphology, LULC and so on (Tehrany et al., 2015). Besides, all the factors may not be accommodating into a particular model; in addition, all the factors may not contribute to FS models. So, the selection of effective FS factors following proper and scientific method is one of the vital and primary works in this regard. In this study, on the basis of previous studies, suitable FS factors were taken into consideration. FS mapping of the study has been done applying selected models. Model verification was done using AUC, and it has been found that LR performed best compared to FL, FR and MCDA. Consequently, this study found that FS applying the LR model is more dependable compared to other MCDA methods (FL, FR and MCDA). This is quite evident that LR outperforms the other MCDA method (Fig. 5) as LR can analyze the multiple factors of an event in a statistically sound way, whereas MCDA only considered the weights given by human who is supposed to be always associated with some biases (Guitouni & Martel, 1998; Roy & Vanderpooten, 1996; Thokala et al., 2016). Besides this, MCDA is hugely depended on the accessibility of the data (Guitouni & Martel, 1998; Thokala et al., 2016). The study by (Chakraborty & Mukhopadhyay, 2019) in the Coochbehar district of West Bengal (Kanani-Sadat et al., 2019) in the Kurdistan Province of Iran and (Souissi et al., 2019) in the arid areas of southeast Tunisia found that MCDA model is very successful with an AUC value of 89.64%, 91.8% and 74.51%, respectively, whereas this study found that the accuracy level of the MCDA model was 86.9%. (Nandalal & Ratnayake, 2011) studied on the forest and agriculture dominated Kalu-Ganga catchment of Sri Lanka, stated that FL is more suitable with very good accuracy. But the findings of (Tehrany & Kumar, 2018) stated that LR performed better than the statistical models. Besides, LR was able to forecast FS 79.45% accurately. Similarly, studies by (Nandi et al., 2016) and (Pham et al., 2020) depict that LR was greatly fruitful to forecast FS effectively 78.9% and 76% correspondingly. It was observed that elevation, plane curvature, older alluvium (Sijua formation) and recent alluvium (Chinsura formation) were very much dominating in the prediction of FS and its coefficients are as follows 19.078, 18.547, 15.952 and 16.174, respectively, whereas SPI (-0.443), aspect (-0.001), rainfall (-0.01) are the minimum effective for FS. So, the rainfall coefficient is very low, because the rainfall over the FS is not effectively responsible, but rainfall in the middle and upper part is the key reason for the occurrences of floods in this area.

Water-related information is very crucial to manage the water resource (Mohammadi et al., 2020; Mohammadi, Guan, et al., 2020; Mohammadi, Linh, et al., 2020). Several measures were proposed below in this section, which can be considered in flood management. For example, numerous anthropogenic activities alter the channel morphology of the river and are narrowing the channel capacities mostly after the independence (Malik & Pal, 2020b, 2020c, 2020d). It was observed that the alignment of the embankment is extremely close to the active channel (Malik & Pal, 2020c). Numerous palaeo-channels have been

found in the lower part of the Dwarkeswar River as well. So, these palaeo-channels should be renovated to provide an extra channel to pass the excessive flow in the main channel as well as to provide an additional water holding capacity to the floodplain. As well as, human encroachment in the form of should be restricted particularly near the river and appropriate assessment should be done before building any type of engineering construction on the river. Along with this, the study area is only associated with three river gauge height recording stations, and thus, it is very essential to increase the number of river flow monitoring stations equipped with modern instruments. The future prediction of flood inundation area and duration can be estimated through real-time monitoring. This will also help in taking required actions before the flood, during the flood and after the flood to manage the entire flood situation more effectively. Based on the flood frequency analysis (Malik & Pal, 2021) and FS map, LULC of the study area can be planned to reduce the flood effects. For example, an area with very high flood risk should be devoid of permanent settlements, and therefore, rehabilitation of the people from the high-risk zone to the comparatively low-risk zone can be done. Besides this, the structure of the house should be made keeping the view of historical flood height records in mind. Digging of new ponds and small water tank and their renovations should be implemented all over the river basin to reduce the flash flow of the river (Malik & Pal, 2020a). Besides, afforestation of bare surface with aboriginal plant species may also be proved to be an important way to reduce the lag time (Malik & Pal, 2020a). Apart from this, the crops, animal and human lives should be secured by different insurance policies which can help them to survive after any natural hazard. In this case, the local administrative bodies can play a very crucial role by enlisting all the needy people.

The outcome of the current work will be very beneficial to assess the FS, and thus, it will provide the basic needs of the policymakers and planners to identify, manage and reduce the impact of the flood with effective strategies in the DRB. However, it may also be applicable to the similar part of the Bengal Basin and other areas of the world. It will also help the investigators to select appropriate methods to analyze the FS of any area. Besides this, it may also be helpful for several Government Organizations, NGOs and academicians. Lack of spatiotemporal variation of flooded and rainfall data was the major limitation of the study. Another limitation of this study is that the FS map is only able to show the spatial extension of the flood rather than a spatial variation of flood depth and its velocity. So, a future study on the flood depth and its velocity in combination with various established hydrological models can be done.

6 Conclusion

In this study, MCDA and LR such as FL, APH and FR methods have been applied to assess the FS mapping of the Dhalkishore or Dwarkeswar River. Sixteen topographic and flood causative factors have been selected based on the FI datasets from earlier research works, and spatial databases were generated in the GIS environment to build the models. Multi-collinearity test has been used, and less than 5 VIF value has been considered as a threshold limit to avoid the multi-collinearity issue. The collected flood inventory data points were classified into two sets. Seventy percentage of the data were used as a model data input, and the remaining thirty percentage of the data were used for validation purposes using AUC. The MCDA model shows that 12.37%, 18.92%, 22.99%, 22.28% and 23.44% area of the basin is under very low, low, moderate, high and very high FS correspondingly. The FL model indicates that 17.29%, 23.02%, 20.25%, 19.90% and 19.54% area of the

basin is under the very high, high, moderate, low and very low category of FS. Also, the FR model represents 24.16%, 21.55%, 22.99%, 24.27% and 7.02% very high, high, moderate, low and very low FS. On the other hand, LR predicts that 30.89%, 20.59%, 16.80%, 16.69% and 15.02% area of the basin is susceptible to very low, low, moderate, high and very high flood probability. According to the AUC test results, the AUC values of the selected models such as FL, MCDA, FR and LR are 0.893, 0.857, 0.835 and 0.916, respectively. So, the LR is more reliable compared to the MCDA, FL and FR in FS analysis. FS map using LR shows that 15.02% and 16.69% areas of the river basin are under the very high and high susceptible zones, respectively, which are mainly placed at the lower portion of the basin characterized by flat alluvial surface. According to the LR model, the elevation is the most dominating flood-controlling factors. Besides, the TWI, plane curvature, water body and geology were playing a dominating role in the prediction of FS map with coefficient value of greater than 15. So, this map can help the policymakers to prepare sound planning to reduce flood damages and human deaths in future in this area as well as the rest of the world. Major limitations of this study are the lack of all historical flood records, limited non-flood points and flood point's data were used along with this all the models were not able to predict the FS 100% as the nature is very dynamic.

Author contributions No other author is associated with this work. The authors would also like to thank the Editor and three anonymous reviewers for their encouraging comments.

Declarations

Conflict of interest There is no conflict of interest among the authors regarding this work.

References

- Al-Juaidi, A. E. M., Nassar, A. M., & Al-Juaidi, O. E. M. (2018). Evaluation of flood susceptibility mapping using logistic regression and GIS conditioning factors. *Arabian Journal of Geosciences*, *11*(24), 765. <https://doi.org/10.1007/s12517-018-4095-0>.
- Arabameri, A., Karimi-Sangchini, E., Pal, S. C., Saha, A., Chowdhuri, I., Lee, S., & Tien Bui, D. (2020a). Novel Credal Decision Tree-Based Ensemble Approaches for Predicting the Landslide Susceptibility. *Remote Sensing*, *12*(20), 3389. <https://doi.org/10.3390/rs12203389>.
- Arabameri, A., Pradhan, B., & Lombardo, L. (2019a). Comparative assessment using boosted regression trees, binary logistic regression, frequency ratio and numerical risk factor for gully erosion susceptibility modelling. *CATENA*, *183*, 104223. <https://doi.org/10.1016/j.catena.2019.104223>.
- Arabameri, A., Pradhan, B., Rezaei, K., & Lee, C. W. (2019). Assessment of landslide susceptibility using statistical- and artificial intelligence-based FR-RF integrated model and multiresolution DEMs. *Remote Sensing*, *11*(9), 999. <https://doi.org/10.3390/rs11090999>.
- Arabameri, A., Saha, S., Mukherjee, K., Blaschke, T., Chen, W., Ngo, P. T. T., & Band, S. S. (2020). Modeling Spatial Flood using Novel Ensemble Artificial Intelligence Approaches in Northern Iran. *Remote Sensing*, *12*(20), 3423. <https://doi.org/10.3390/rs12203423>.
- Band, S. S., Janizadeh, S., Chandra Pal, S., Saha, A., Chakraborty, R., Melesse, A. M., & Mosavi, A. (2020). Flash Flood Susceptibility Modeling Using New Approaches of Hybrid and Ensemble Tree-Based Machine Learning Algorithms. *Remote Sensing*, *12*(21), 3568. <https://doi.org/10.3390/rs12213568>.
- Bandyopadhyay, S., Ghosh, P. K., Jana, N. C., & Sinha, S. (2016). Probability of flooding and vulnerability assessment in the Ajay River, Eastern India: implications for mitigation. *Environmental Earth Sciences*, *75*(7), 578. <https://doi.org/10.1007/s12665-016-5297-y>.
- Bonham-Carter, G. F. (1994). Geographic information systems for geoscientists-modeling with GIS. *Computer methods in the geosciences*, *13*, 398.

- Brammer, H. (2010). After the Bangladesh flood action plan: looking to the future. *Environmental Hazards*, 9(1), 118–130.
- Chakraborty, R., Pal, S. C., Malik, S., & Das, B. (2018). Modeling and mapping of groundwater potentiality zones using AHP and GIS technique: a case study of Raniganj Block, Paschim Bardhaman, West Bengal. *Modeling Earth Systems and Environment*, 4(3), 1085–1110. <https://doi.org/10.1007/s40808-018-0471-8>.
- Chakraborty, S., & Mukhopadhyay, S. (2019). Assessing flood risk using analytical hierarchy process (AHP) and geographical information system (GIS): application in Coochbehar district of West Bengal. *India. Natural Hazards*, 99(1), 247–274. <https://doi.org/10.1007/s11069-019-03737-7>.
- Chapi, K., Singh, V. P., Shirzadi, A., Shahabi, H., Bui, D. T., Pham, B. T., & Khosravi, K. (2017). A novel hybrid artificial intelligence approach for flood susceptibility assessment. *Environmental Modelling & Software*, 95, 229–245. <https://doi.org/10.1016/j.envsoft.2017.06.012>.
- Chapman, G. P., & Rudra, K. (2007). Water as Foe, Water as Friend: Lessons from Bengal's Millennium Flood. *Journal of South Asian Development*, 2(1), 19–49. <https://doi.org/10.1177/097317410600200102>.
- Chen, W., Li, Y., Xue, W., Shahabi, H., Li, S., Hong, H., et al. (2020). Modeling flood susceptibility using data-driven approaches of naïve bayes tree, alternating decision tree, and random forest methods. *Science of The Total Environment*, 701, 134979.
- Choubin, B., Moradi, E., Golshan, M., Adamowski, J., Sajedi-Hosseini, F., & Mosavi, A. (2019). An ensemble prediction of flood susceptibility using multivariate discriminant analysis, classification and regression trees, and support vector machines. *Science of the Total Environment*, 651, 2087–2096. <https://doi.org/10.1016/j.scitotenv.2018.10.064>.
- Chowdhuri, I., Pal, S. C., Arabameri, A., Saha, A., Chakraborty, R., Blaschke, T., et al. (2020). Implementation of Artificial Intelligence Based Ensemble Models for Gully Erosion Susceptibility Assessment. *Remote Sensing*, 12(21), 3620. <https://doi.org/10.3390/rs12213620>.
- Chowdhuri, I., Pal, S. C., & Chakraborty, R. (2020). Flood susceptibility mapping by ensemble evidential belief function and binomial logistic regression model on river basin of eastern India. *Advances in Space Research*, 65(5), 1466–1489. <https://doi.org/10.1016/j.asr.2019.12.003>.
- Christensen, J. H., & Christensen, O. B. (2003). Severe summertime flooding in Europe. *Nature*, 421(6925), 805–806. <https://doi.org/10.1038/421805a>.
- Costabile, P., & Macchione, F. (2015). Enhancing river model set-up for 2-D dynamic flood modelling. *Environmental Modelling and Software*, 67, 89–107. <https://doi.org/10.1016/j.envsoft.2015.01.009>.
- Costache, R., Arabameri, A., Blaschke, T., Pham, Q. B., Pham, B. T., Pandey, M., et al. (2021). Flash-Flood Potential Mapping Using Deep Learning, Alternating Decision Trees and Data Provided by Remote Sensing Sensors. *Sensors*, 21(1), 280.
- Dano, U. L., Balogun, A.-L., Matori, A.-N., Wan Yusouf, K., Abubakar, I. R., Said Mohamed, M. A., et al. (2019). Flood Susceptibility Mapping Using GIS-Based Analytic Network Process: A Case Study of Perlis. *Malaysia. Water*, 11(3), 615. <https://doi.org/10.3390/w11030615>.
- Das, B., Pal, S. C., & Malik, S. (2018). Assessment of flood hazard in a riverine tract between Damodar and Dwarakeswar River, Hugli District, West Bengal. *India. Spatial Information Research*, 26(1), 91–101. <https://doi.org/10.1007/s41324-017-0157-8>.
- Dottori, F., Martina, M. L. V., & Figueiredo, R. (2018). A methodology for flood susceptibility and vulnerability analysis in complex flood scenarios. *Journal of Flood Risk Management*, 11, S632–S645. <https://doi.org/10.1111/jfr3.12234>.
- Ergu, D., Kou, G., Peng, Y., & Shi, Y. (2011). A simple method to improve the consistency ratio of the pairwise comparison matrix in ANP. *European Journal of Operational Research*, 213(1), 246–259.
- Falah, F., Rahmati, O., Rostami, M., Ahmadisharaf, E., Daliakopoulos, I. N., & Pourghasemi, H. R. (2019). Artificial Neural Networks for Flood Susceptibility Mapping in Data-Scarce Urban Areas. In H. R. Moradi, M. T. Avand, & S. Janzadeh (Eds.), *Spatial Modeling in GIS and R for Earth and Environmental Sciences*. (pp. 323–336). Amsterdam: Elsevier.
- Fernández, D. S., & Lutz, M. A. (2010). Urban flood hazard zoning in Tucumán Province, Argentina, using GIS and multicriteria decision analysis. *Engineering Geology*, 111(1–4), 90–98. <https://doi.org/10.1016/j.enggeo.2009.12.006>.
- Ganguly, S., Samanta, A., Schull, M. A., Shabanov, N. V., Milesi, C., Nemani, R. R., et al. (2008). Generating vegetation leaf area index Earth system data record from multiple sensors. Part 2: Implementation, analysis and validation. *Remote Sensing of Environment*, 112(12), 4318–4332. <https://doi.org/10.1016/J.RSE.2008.07.013>.
- GSI. (1999). Geology and Mineral Resources of the States of India, Pt. 1: West Bengal, Misc. Publ., India.
- Guitouni, A., & Martel, J.-M. (1998). Tentative guidelines to help choosing an appropriate MCDA method. *European journal of operational research*, 109(2), 501–521.

- Hagen, E., & Lu, X. X. (2011). Let us create flood hazard maps for developing countries. *Natural Hazards*, 58(3), 841–843. <https://doi.org/10.1007/s11069-011-9750-7>.
- Haghizadeh, A., Siahkamari, S., Haghbi, A. H., & Rahmati, O. (2017). Forecasting flood-prone areas using Shannon's entropy model. *Journal of Earth System Science*. <https://doi.org/10.1007/s12040-017-0819-x>.
- Horton, R. E. (1932). Drainage Basin Characteristics. *Eos, Transactions American Geophysical Union*, 13(1), 350–361. <https://doi.org/10.1029/TR013i001p00350>.
- Huang, X., Tan, H., Zhou, J., Yang, T., Benjamin, A., Wen, S. W., et al. (2008). Flood hazard in Hunan province of China: An economic loss analysis. *Natural Hazards*, 47(1), 65–73. <https://doi.org/10.1007/s11069-007-9197-z>.
- Irrigation and Waterways Directorate Govt. of West Bengal. (2016). *Annual Flood Report, 2016*. Kolkata.
- Kadam, P., & Sen, D. (2012). Flood inundation simulation in Ajoy River using MIKE-FLOOD. *ISH Journal of Hydraulic Engineering*, 18(2), 129–141. <https://doi.org/10.1080/09715010.2012.695449>.
- Kale, V. S. (2003). *The spatio-temporal aspects of monsoon floods in India: Implications for flood hazard management*. (pp. 22–47). Universities Press, Hyderabad.
- Kale, V. S. (2003). Geomorphic effects of monsoon floods on Indian rivers. *Natural Hazards*, 28(1), 65–84. <https://doi.org/10.1023/A:1021121815395>.
- Kale, V. S. (2014). Is flooding in South Asia getting worse and more frequent? *Singapore Journal of Tropical Geography*, 35(2), 161–178. <https://doi.org/10.1111/sjtg.12060>.
- Kanani-Sadat, Y., Arabsheibani, R., Karimpour, F., & Nasser, M. (2019). A new approach to flood susceptibility assessment in data-scarce and ungauged regions based on GIS-based hybrid multi criteria decision-making method. *Journal of Hydrology*, 572, 17–31. <https://doi.org/10.1016/j.jhydrol.2019.02.034>.
- Khosravi, K., Shahabi, H., Pham, B. T., Adamowski, J., Shirzadi, A., Pradhan, B., et al. (2019). A comparative assessment of flood susceptibility modeling using Multi-Criteria Decision-Making Analysis and Machine Learning Methods. *Journal of Hydrology*, 573, 311–323. <https://doi.org/10.1016/j.jhydrol.2019.03.073>.
- Kourgialas, N. N., & Karatzas, G. P. (2011). Flood management and a GIS modelling method to assess flood-hazard areas—a case study. *Hydrological Sciences Journal*, 56(2), 212–225. <https://doi.org/10.1080/02626667.2011.555836>.
- Kumar, R., & Acharya, P. (2016). Flood hazard and risk assessment of 2014 floods in Kashmir Valley: a space-based multisensor approach. *Natural Hazards*, 84(1), 437–464. <https://doi.org/10.1007/s11069-016-2428-4>.
- Lee, M. J., Kang, J. E., & Jeon, S. (2012). Application of frequency ratio model and validation for predictive flooded area susceptibility mapping using GIS. In *International Geoscience and Remote Sensing Symposium (IGARSS)* (pp. 895–898). <https://doi.org/https://doi.org/10.1109/IGARSS.2012.6351414>
- Lee, S., & Sambath, T. (2006). Landslide susceptibility mapping in the Damrei Romel area, Cambodia using frequency ratio and logistic regression models. *Environmental Geology*, 50(6), 847–855.
- Lee, S., Kim, J.-C., Jung, H.-S., Lee, M. J., & Lee, S. (2017). Spatial prediction of flood susceptibility using random-forest and boosted-tree models in Seoul metropolitan city, Korea. *Geomatics, Natural Hazards and Risk*, 8(2), 1185–1203.
- Lin, L., Wu, Z., & Liang, Q. (2019). Urban flood susceptibility analysis using a GIS-based multi-criteria analysis framework. *Natural Hazards*, 97(2), 455–475. <https://doi.org/10.1007/s11069-019-03615-2>.
- Ma, Z., Qin, S., Cao, C., Lv, J., Li, G., Qiao, S., & Hu, X. (2019). The influence of different knowledge-driven methods on landslide susceptibility mapping: A case study in the Changbai Mountain Area, Northeast China. *Entropy*, 21(4). <https://doi.org/https://doi.org/10.3390/e21040372>
- Madani, A. A. (2011). Knowledge-driven GIS modeling technique for gold exploration, Bulghah gold mine area, Saudi Arabia. *Egyptian Journal of Remote Sensing and Space Science*, 14(2), 91–97. <https://doi.org/10.1016/j.ejrs.2011.10.001>.
- Malik, S., Chandra Pal, S., Chowdhuri, I., Chakraborty, R., Roy, P., & Das, B. (2020). Prediction of highly flood prone areas by GIS based heuristic and statistical model in a monsoon dominated region of Bengal Basin. *Remote Sensing Applications: Society and Environment*, 19, 100343. <https://doi.org/10.1016/j.rsase.2020.100343>.
- Malik, S., & Pal, S. C. (2020). Application of 2D numerical simulation for rating curve development and inundation area mapping: a case study of monsoon dominated Dwarkeswar river. *International Journal of River Basin Management*. <https://doi.org/10.1080/15715124.2020.1738447>.

- Malik, S., & Pal, S. C. (2020). Downstream Decreasing Channel Capacity of a Monsoon-dominated Bengal Basin River: A Case Study of Dwarakeswar River. *Eastern India. Chinese Geographical Science*. <https://doi.org/10.1007/s11769-020-1143-y>.
- Malik, S., & Pal, S. C. (2020). Anthropogenic Impact on Channel and Extra-Channel Geomorphology of the Dwarakeswar River Basin. In B. C. Das, S. Ghosh, A. Islam, & S. Roy (Eds.), *Anthropogeomorphology of Bhagirathi-Hooghly River System in India*. Florida: CRC Press.
- Malik, S., & Pal, S. C. (2020). Is the topography playing a dual role in controlling downstream channel morphology of a monsoon dominated Dwarakeswar River, Eastern India? *HydroResearch*, 3, 15–31. <https://doi.org/10.1016/j.hydrres.2020.04.002>.
- Malik, S., & Pal, S. C. (2021). Potential flood frequency analysis and susceptibility mapping using CMIP5 of MIROC5 and HEC-RAS model: a case study of lower Dwarakeswar River, Eastern India. *SN Applied Sciences*. <https://doi.org/10.1007/s42452-020-04104-z>.
- Malik, S., Pal, S. C., Das, B., & Chakraborty, R. (2019). Assessment of vegetation status of Sali River basin, a tributary of Damodar River in Bankura District, West Bengal, using satellite data. *Environment, Development and Sustainability*. <https://doi.org/10.1007/s10668-019-00444-y>.
- Malik, S., Pal, S. C., Sattar, A., Singh, S. K., Das, B., Chakraborty, R., & Mohammad, P. (2020). Trend of extreme rainfall events using suitable Global Circulation Model to combat the water logging condition in Kolkata Metropolitan Area. *Urban Climate*, 32, 100599. <https://doi.org/10.1016/j.uclim.2020.100599>.
- Mandal, S. P., Chakrabarty, A., & Maity, P. (2018). Comparative evaluation of information value and frequency ratio in landslide susceptibility analysis along national highways of Sikkim Himalaya. *Spatial Information Research*, 26(2), 127–141.
- Markantonis, V., Meyer, V., & Lienhoop, N. (2013). Evaluation of the environmental impacts of extreme floods in the Evros River basin using Contingent Valuation Method. *Natural Hazards*, 69(3), 1535–1549. <https://doi.org/10.1007/s11069-013-0762-3>.
- Miller, J. R., Ritter, D. F., & Kochel, R. C. (1990). Morphometric assessment of lithologic controls on drainage basin evolution in the Crawford Upland, south-central Indiana. *American Journal of Science*, 290(5), 569–599. <https://doi.org/10.2475/ajs.290.5.569>.
- Mind'je, R., Li, L., Amanambu, A. C., Nahayo, L., Nsengiyumva, J. B., Gasirabo, A., & Mindje, M. (2019). Flood susceptibility modeling and hazard perception in Rwanda. *International Journal of Disaster Risk Reduction*, 38, 101211. <https://doi.org/10.1016/j.ijdrr.2019.101211>.
- Minh, P. T., Tuyet, B. T., Thao, T., & Hang, L. T. (2018). Application of ensemble Kalman filter in WRF model to forecast rainfall on monsoon onset period in South Vietnam. *Vietnam Journal of Earth Sciences*, 40(4), 367–394. <https://doi.org/10.15625/0866-7187/40/4/13134>.
- Mirza, M. M. Q. (2011). Climate change, flooding in South Asia and implications. *Regional Environmental Change*, 11(S1), 95–107. <https://doi.org/10.1007/s10113-010-0184-7>.
- Mohammadi, B., Ahmadi, F., Mehdizadeh, S., Guan, Y., Pham, Q. B., Linh, N. T. T., & Tri, D. Q. (2020). Developing Novel Robust Models to Improve the Accuracy of Daily Streamflow Modeling. *Water Resources Management*, 34(10), 3387–3409. <https://doi.org/10.1007/s11269-020-02619-z>.
- Mohammadi, B., Guan, Y., Aghelpour, P., Emamgholizadeh, S., Zolá, R. P., & Zhang, D. (2020). Simulation of titicaca lake water level fluctuations using hybrid machine learning technique integrated with grey wolf optimizer algorithm. *Water (Switzerland)*, 12(11), 1–18. <https://doi.org/10.3390/w12113015>.
- Mohammadi, B., Linh, N. T. T., Pham, Q. B., Ahmed, A. N., Vojteková, J., Guan, Y., et al. (2020). Adaptive neuro-fuzzy inference system coupled with shuffled frog leaping algorithm for predicting river streamflow time series. *Hydrological Sciences Journal*, 65(10), 1738–1751. <https://doi.org/10.1080/02626667.2020.1758703>.
- Mukerji, A., Chatterjee, C., & Raghuvanshi, N. S. (2009). Flood Forecasting Using ANN, Neuro-Fuzzy, and Neuro-GA Models. *Journal of Hydrologic Engineering*, 14(6), 647–652. [https://doi.org/10.1061/\(asce\)he.1943-5584.0000040](https://doi.org/10.1061/(asce)he.1943-5584.0000040).
- Nachappa, T. G., Piralilou, S. T., Gholamnia, K., Ghorbanzadeh, O., Rahmati, O., & Blaschke, T. (2020). Flood susceptibility mapping with machine learning, multi-criteria decision analysis and ensemble using Dempster Shafer Theory. *Journal of Hydrology*, 11(1), 2147–2175.
- Najafzadeh, M., & Zahiri, A. (2015). Neuro-Fuzzy GMDH-Based Evolutionary Algorithms to Predict Flow Discharge in Straight Compound Channels. *Journal of Hydrologic Engineering*, 20(12), 04015035. [https://doi.org/10.1061/\(asce\)he.1943-5584.0001185](https://doi.org/10.1061/(asce)he.1943-5584.0001185).
- Nandalal, H. K., & Ratnayake, U. R. (2011). Flood risk analysis using fuzzy models. *Journal of Flood Risk Management*, 4(2), 128–139. <https://doi.org/10.1111/j.1753-318X.2011.01097.x>.
- Nandi, A., Mandal, A., Wilson, M., & Smith, D. (2016). Flood hazard mapping in Jamaica using principal component analysis and logistic regression. *Environmental Earth Sciences*, 75(6), 465.
- O'Malley, L. S. S. (1995). *Bengal District Gazetteers Bankura*. Government of West Bengal.

- Pal, S. C., Arabameri, A., Blaschke, T., Chowdhuri, I., Saha, A., Chakraborty, R., et al. (2020). Ensemble of Machine-Learning Methods for Predicting Gully Erosion Susceptibility. *Remote Sensing*, *12*(22), 3675. <https://doi.org/10.3390/rs12223675>.
- Pal, S. C., & Chowdhuri, I. (2019). GIS-based spatial prediction of landslide susceptibility using frequency ratio model of Lachung River basin, North Sikkim, India. *SN Applied Sciences*, *1*(5), 1–25. <https://doi.org/10.1007/s42452-019-0422-7>.
- Paul, G. C., Saha, S., & Hembram, T. K. (2019). Application of the GIS-Based Probabilistic Models for Mapping the Flood Susceptibility in Bansloi Sub-basin of Ganga-Bhagirathi River and Their Comparison. *Remote Sensing in Earth Systems Sciences*, *2*(2–3), 120–146. <https://doi.org/10.1007/s41976-019-00018-6>.
- Pham, B. T., Phong, T. V., Nguyen, H. D., Qi, C., Al-Ansari, N., Amini, A., et al. (2020). A comparative study of kernel logistic regression, radial basis function classifier, multinomial naïve bayes, and logistic model tree for flash flood susceptibility mapping. *Water*, *12*(1), 239.
- Pourghasemi, H. R., & Beheshtirad, M. (2015). Assessment of a data-driven evidential belief function model and GIS for groundwater potential mapping in the Koohrang Watershed. *Iran. Geocarto International*, *30*(6), 662–685. <https://doi.org/10.1080/10106049.2014.966161>.
- Pourghasemi, H. R., & Rahmati, O. (2018). Prediction of the landslide susceptibility: Which algorithm, which precision? *CATENA*, *162*, 177–192. <https://doi.org/10.1016/j.catena.2017.11.022>.
- Pradhan, B., & Youssef, A. M. (2011). A 100-year maximum flood susceptibility mapping using integrated hydrological and hydrodynamic models: Kelantan River Corridor. *Malaysia. Journal of Flood Risk Management*, *4*(3), 189–202. <https://doi.org/10.1111/j.1753-318X.2011.01103.x>.
- Pulvirenti, L., Pierdicca, N., Chini, M., & Guerriero, L. (2011). An algorithm for operational flood mapping from Synthetic Aperture Radar (SAR) data using fuzzy logic. *Natural Hazards and Earth System Sciences*, *11*(2), 529–540.
- Rahmati, O., Pourghasemi, H. R., & Zeinivand, H. (2016). Flood susceptibility mapping using frequency ratio and weights-of-evidence models in the Golastan Province. *Iran. Geocarto International*, *31*(1), 42–70. <https://doi.org/10.1080/10106049.2015.1041559>.
- Rahmati, O., Zeinivand, H., & Besharat, M. (2016). Flood hazard zoning in Yasooj region, Iran, using GIS and multi-criteria decision analysis. *Geomatics, Natural Hazards and Risk*, *7*(3), 1000–1017. <https://doi.org/10.1080/19475705.2015.1045043>.
- Ray, P. K. C., Dimri, S., Lakhera, R. C., & Sati, S. (2007). Fuzzy-based method for landslide hazard assessment in active seismic zone of Himalaya. *Landslides*, *4*(2), 101–111. <https://doi.org/10.1007/s10346-006-0068-6>.
- RMSI. (2015). *India FloodRisk India's First Countrywide Flood Risk Model*. Retrieved from https://www.rmsi.com/uploads/Services/IndiaFloodRisk_Jan15.pdf.
- Roy, B., & Vanderpooten, D. (1996). The European school of MCDA: Emergence, basic features and current works. *Journal of Multi-Criteria Decision Analysis*, *5*(1), 22–38.
- Roy, P., Chandra Pal, S., Chakraborty, R., Chowdhuri, I., Malik, S., & Das, B. (2020). Threats of climate and land use change on future flood susceptibility. *Journal of Cleaner Production*, *272*, 122757. <https://doi.org/10.1016/j.jclepro.2020.122757>.
- Saaty, T. L. (1977). A scaling method for priorities in hierarchical structures. *Journal of Mathematical Psychology*, *15*(3), 234–281. [https://doi.org/10.1016/0022-2496\(77\)90033-5](https://doi.org/10.1016/0022-2496(77)90033-5).
- Saha, A., Pal, S. C., Arabameri, A., Blaschke, T., Panahi, S., Chowdhuri, I., et al. (2021). Flood Susceptibility Assessment Using Novel Ensemble of Hyperpipes and Support Vector Regression Algorithms. *Water*, *13*(2), 241. <https://doi.org/10.3390/w13020241>.
- Sahana, M., & Patel, P. P. (2019). A comparison of frequency ratio and fuzzy logic models for flood susceptibility assessment of the lower Kosi River Basin in India. *Environmental Earth Sciences*. <https://doi.org/10.1007/s12665-019-8285-1>.
- Samanta, S., Pal, D. K., & Palsamanta, B. (2018). Flood susceptibility analysis through remote sensing, GIS and frequency ratio model. *Applied Water Science*, *8*(2), 1–14.
- Shafapour Tehrani, M., Kumar, L., Neamah Jebur, M., & Shabani, F. (2019). Evaluating the application of the statistical index method in flood susceptibility mapping and its comparison with frequency ratio and logistic regression methods. *Geomatics, Natural Hazards and Risk*, *10*(1), 79–101. <https://doi.org/10.1080/19475705.2018.1506509>.
- Smith, K. (2013). *Environmental Hazards: assessing risk and reducing disaster*. (4th ed.). England: Routledge.
- SOI. (1978). *Topographical Map from Survey of India*. Government of India.
- Solomatine, D. P., & Ostfeld, A. (2008). Data-driven modelling: Some past experiences and new approaches. *Journal of Hydroinformatics*, *10*, 3–22. <https://doi.org/10.2166/hydro.2008.015>.

- Souissi, D., Zouhri, L., Hammami, S., Msaddek, M. H., Zghibi, A., & Dlala, M. (2019). GIS-based MCDM–AHP modeling for flood susceptibility mapping of arid areas, southeastern Tunisia. *Geocarto International*. <https://doi.org/10.1080/10106049.2019.1566405>.
- Souissi, D., Zouhri, L., Hammami, S., Msaddek, M. H., Zghibi, A., & Dlala, M. (2020). GIS-based MCDM–AHP modeling for flood susceptibility mapping of arid areas, southeastern Tunisia. *Geocarto International*, 35(9), 991–1017.
- Strahler, A. N. (1957). Quantitative analysis of watershed geomorphology. *Transactions, American Geophysical Union*, 38(6), 913. <https://doi.org/10.1029/TR038i006p00913>.
- Swain, K. C., Singha, C., & Nayak, L. (2020). Flood Susceptibility Mapping through the GIS-AHP Technique Using the Cloud. *ISPRS International Journal of Geo-Information*, 9(12), 720.
- Tang, X., Li, J., Liu, M., Liu, W., & Hong, H. (2020). Flood susceptibility assessment based on a novel random Naïve Bayes method: A comparison between different factor discretization methods. *CATENA*, 190, 104536.
- Tehrany, M. S., & Kumar, L. (2018). The application of a Dempster–Shafer-based evidential belief function in flood susceptibility mapping and comparison with frequency ratio and logistic regression methods. *Environmental Earth Sciences*. <https://doi.org/10.1007/s12665-018-7667-0>.
- Tehrany, M. S., Pradhan, B., & Jebur, M. N. (2014). Flood susceptibility mapping using a novel ensemble weights-of-evidence and support vector machine models in GIS. *Journal of Hydrology*, 512, 332–343. <https://doi.org/10.1016/j.jhydrol.2014.03.008>.
- Tehrany, M. S., Pradhan, B., & Jebur, M. N. (2015). Flood susceptibility analysis and its verification using a novel ensemble support vector machine and frequency ratio method. *Stochastic Environmental Research and Risk Assessment*, 29(4), 1149–1165. <https://doi.org/10.1007/s00477-015-1021-9>.
- Termeh, S. V. R., Kornejady, A., Pourghasemi, H. R., & Keesstra, S. (2018). Flood susceptibility mapping using novel ensembles of adaptive neuro fuzzy inference system and metaheuristic algorithms. *Science of the Total Environment*, 615, 438–451.
- Thakur, P., & Chauhan, N. (2018, June). Delhi most vulnerable UT in India's first disaster risk index Maharashtra Leads States. *Times of India*, p. Online Publication: <https://timesofindia.indiatime>. New Delhi.
- Thokala, P., Devlin, N., Marsh, K., Baltussen, R., Boysen, M., Kalo, Z., et al. (2016). Multiple criteria decision analysis for health care decision making—an introduction: report 1 of the ISPOR MCDA Emerging Good Practices Task Force. *Value in health*, 19(1), 1–13.
- Van Balen, R. T., Busschers, F. S., & Tucker, G. E. (2010). Geomorphology Modeling the response of the Rhine – Meuse fluvial system to Late Pleistocene climate change. *Geomorphology*, 114(3), 440–452. <https://doi.org/10.1016/j.geomorph.2009.08.007>.
- Van Tu, T., Duc, D. M., Tung, N. M., & Cong, V. D. (2016). Preliminary assessments of debris flow hazard in relation to geological environment changes in mountainous regions North Vietnam. *Vietnam Journal of Earth Sciences*. <https://doi.org/10.15625/0866-7187/38/3/8712>.
- Wheater, H., Jakeman, A., & Beven, K. (1993). *Progress and directions in rainfall-runoff modelling*. . New Jersey: Wiley.
- WMO. (2018). *2018 Annual Report: WMO for the Twenty-first Century*.
- Yesilnacar, E., & Topal, T. (2005). Landslide susceptibility mapping: A comparison of logistic regression and neural networks methods in a medium scale study, Hendek region (Turkey). *Engineering Geology*, 79(3–4), 251–266. <https://doi.org/10.1016/j.enggeo.2005.02.002>.
- Yilmaz, I. (2010). Comparison of landslide susceptibility mapping methodologies for Koyulhisar, Turkey: Conditional probability, logistic regression, artificial neural networks, and support vector machine. *Environmental Earth Sciences*, 61(4), 821–836. <https://doi.org/10.1007/s12665-009-0394-9>.
- Zadeh, L. (1965). Fuzzy sets. *Inf. Control*, 8, 253–338.
- Zahiri, A., & Najafzadeh, M. (2018). Optimized expressions to evaluate the flow discharge in main channels and floodplains using evolutionary computing and model classification. *International Journal of River Basin Management*, 16(1), 123–132. <https://doi.org/10.1080/15715124.2017.1372448>.
- Zheng, X., Maidment, D. R., Tarboton, D. G., Liu, Y. Y., & Passalacqua, P. (2018). GeoFlood: Large-Scale Flood Inundation Mapping Based on High-Resolution Terrain Analysis. *Water Resources Research*, 54(12), 10013–10033. <https://doi.org/10.1029/2018WR023457>.
- Zimmermann, H. (1996). *Fuzzy set theory and its applications* Kluwer Academic Publishers. . New York: Springer.